Cellular and Molecular Neurobiology (2025) 45:47
https://doi.org/10.1007/s10571-025-01566-w

ORIGINAL RESEARCH

Atorvastatin Protects Against the Macrophage/Microglia-Related Neuroinflammation via Inhibiting Lipocalin-2 in Mouse Experimental Intracerebral Hemorrhage Model

Guangming Wang[1] · Hongkang Hu[1] · Junbin Liu[3] · Xiaowei Fei[2] · Yanan Dou[2] · Li Wang[2] · Lin Ying[4] · Guohan Hu[1] · Danfeng Zhang[1] · Lei Jiang[1] · Jialiang Wei[2]

Received: 26 February 2025 / Accepted: 9 May 2025

Abstract

There are few effective pharmacological interventions for intracerebral hemorrhage (ICH). Atorvastatin (Ato) has been shown to exert a substantial protective effect on ischemic stroke and is effective in alleviating neuroinflammation. Lipocalin-2 (LCN2), an important inflammation-regulating protein, has been demonstrated to play pivotal roles in post-ICH neuroinflammation. However, the exact role of Ato and whether LCN2 is involved after ICH remain largely unknown. In the current study, the BV2 (microglia) cell line, which was transfected with or without LCN2 for overexpression/interference, was co-cultured with primary cultured neurons and received blood infusion from C57BL/6 mice in vitro. For the in vivo study, atorvastatin was injected peritoneally into an ICH mouse model, and LCN2 specific knockout using the flox/cre system was performed in mice for mechanism study. Behavioral tests were conducted before ICH and on days 1, 3, and 7 post—ICH, and the brains and cultured cells were collected for protein, histological, and morphological studies. Our results showed that atorvastatin treatment alleviates neural damage and promotes neurological outcomes after ICH. Moreover, M1 activation and pro—inflammatory polarization are inhibited by atorvastatin. In both in vivo and in vitro models, the upregulation of LCN2 after ICH is substantially inhibited by atorvastatin. Studies on LCN2 transgenic mice and LCN2 overexpression/interference cells demonstrated that the suppression of macrophage/microglia (M/M) LCN2 participates in atorvastatin-mediated anti-neuroinflammation and neural protection effects. Therefore, our study suggests that atorvastatin treatment attenuates M/M-related neuroinflammation and protects neural recovery by down—regulating LCN2 after ICH. This study identified a potential novel therapeutic target for ICH treatment.

Guangming Wang, Hongkang Hu and Junbin Liu have contributed equally to this work.

✉ Lei Jiang
czjianglei@163.com; jiangleicz@smmu.edu.cn

✉ Jialiang Wei
weijl@fmmu.edu.cn; kimi_wei@126.com

[1] Department of Neurosurgery, Changzheng Hospital, Naval Medical University, Shanghai, China

[2] Department of Neurosurgery, Xijing Hospital, Fourth Military Medical University, 127 Changlexi Rd, Xi'an, China

[3] Department of Orthopedics, Changzheng Hospital, Naval Medical University, Shanghai, China

[4] College of Basic Medical Sciences, Naval Medical University, Shanghai, China

Published online: 20 May 2025

Graphical Abstract

Atorvastatin treatment counteracts M/M-related neuroinflammation, marked by M1 phenotype marker expression and pro-inflammatory cytokines IL-1β and TNF release, and protects neural recovery, marked by facilitated clot reduction, alleviated neural damage and neurologic functional recovery, after ICH via down-regulation M/M LCN2 expression.

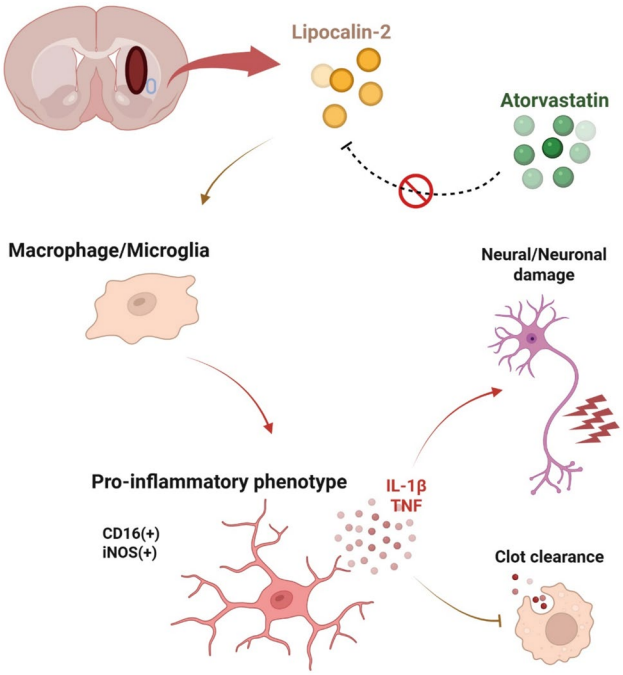

Keywords Intracerebral hemorrhage · Atorvastatin · Macrophage/microglia · Lipocalin-2 · Neuroinflammation

Introduction

Intracerebral hemorrhage (ICH) is the most lethal stroke subtype, characterized by brain vessel rupture. Approximately half of the patients die within one year, and most of them suffer from severe sequelae that seriously affect their quality of life (Puy et al. 2023). Inflammation of the Central nervous system (CNS) is a key factor in brain injury after ICH (Iadecola et al. 2020). As the main immune cells in the CNS, the macrophage/microglia (M/Ms) can polarize into pro- or anti-inflammatory subtype that participate substantially in regulation of neuro-inflammation and neural recovery under various pathophysiological conditions (Yang et al. 2024; Zhao et al. 2015). Our previous studies have shown that the M/Ms play a key role in neuroinflammation induced neural damage as well as neurological rehabilitation after ICH (Wan et al. 2023; Wang et al. 2021; Wei et al. 2022a), indicating a potential therapeutic target for ICH pharmacological treatment.

As a classic clinical drug, atorvastatin plays an important role in the prevention and treatment of heart and stroke diseases (Castellano et al. 2022; Neilan et al. 2023). Researches has shown that the atorvastatin can effectively relieve cognitive impairment, ischemic stroke neuroinflammation (Vizcaychipi et al. 2014; Zhang et al. 2024), and improve microglia function (Goldberg et al. 2024). Also, atorvastatin can effectively improve disease prognosis without increasing the hemorrhage risk in ischemic stroke patients (Gaist et al. 2023; Gao et al. 2024). Although studies have shown that atorvastatin can reduce the incidence of intracerebral hemorrhage (Saliba et al. 2018) and inhibit intracerebral neuroinflammation after subarachnoid hemorrhage (Chen et al. 2021), few researches have focused on the role of atorvastatin on ICH. Although several studies found that the atorvastatin reduces microglia activation, facilitates vascular recovery and improves the neurological outcome after ICH (Chen et al. 2022; Yang et al. 2011; Karki et al. 2009), the optimal dose, as well as the detailed effects and mechanism of atorvastatin in ICH, remain largely unknown.

Research has shown that the atorvastatin can inhibit the expression level of lipocalin-2(LCN2) in vascular diseases (Torrens et al. 2009). Moreover, atorvastatin reduces the serum LCN2 level and improves renal function in patients with kidney disease (Fassett et al. 2012; Kang et al. 2020; Park et al. 2016; Prowle et al. 2012). LCN2 is an important early inflammatory response protein that is upregulated in

different pathological microenvironments (Dekens et al. 2021). LCN2 also participates in the development of various diseases, including myocardial injury after myocardial infarction, non-alcoholic steatohepatitis, and atherosclerotic plaque formation (Hu et al. 2023; Liu et al. 2023; Ye et al. 2016). Additionally, LCN2 has been found to be closely associated with central nervous system diseases such as cognitive impairment and dementia (Li et al. 2023). Our previous researches have shown that the LCN2 participates in neuronal damage and is crucial for M/Ms-mediated neuroinflammation regulation after ICH (Fei et al. 2024; Toyota et al. 2019). However, it remains unclear whether atorvastatin can regulate M/Ms-mediated neuroinflammatory damage after ICH through LCN2.

In the current study, we investigated the effect of atorvastatin treatment on the M/Ms-related neuroinflammation after ICH. Transgenic M/Ms-specific LCN2 knockout mice were used to further explore the mechanism by which atorvastatin regulates M/Ms-related neuroinflammation.

Materials and Methods

Animals

The protocols for animal experiments are approved by the Military Medical University Committee of Animal Use and Care. In the present study, young male C57BL/6 mice aged 18–21 weeks were provided by the Experimental Animal Center of Military Medical University (animal ethics protocol number:#20210424), 8 week-old $LCN2^{f/f,CX3CR1-Cre}$ male mice and $LCN2^{f/f}$ male mice were constructed and incubated by Cyagen Co. (Suzhou, China) (Supplemental data). All mice were housed and randomized following standard protocols as previously described (Wei et al. 2022b), and no more than 5 mice should be raised in each cage. Pre-ICH mice with abnormal corner turns scores or forelimb use asymmetry tests scores were regarded as out-of-order ones and were excluded. The ARRIVE 2.0 guidelines (Supplemental data) were followed for animal data report. Randomization was carried out using odd/even numbers as previously described (Wei et al. 2020).

ICH Modeling

The ICH model in mouse was established as previously described (Wei et al. 2022b). Briefly, the mice were anesthetized using xylazine/ketamine mixtures intraperitoneally with a controlled body temperature of 37 °C. The burr hole was drilled with the coordinates: 2.5 mm lateral and 0.2 mm anterior to the bregma and 30μL autologous blood obtained from the right femoral artery was injected into mice right caudate with the depth of 3.5 mm via a 26-gauge needle (3μL/min). The needle was maintained in situ for extra 10 min before retraction, burr hole sealing and skin suturing.

Cell Culture and Microglia-Neuron Co-culture

The microglial cell line BV2 and primary cultured neurons were used in this study. All cells were cultured at 37 °C in a 5% CO_2 incubator, and the BV2 cell line was cultured using 10% fetal bovine serum (Gibco, #15669701) and high-glucose DMEM (Gibco, #11965118). The primary cultured neurons were obtained and cultured using previously described methods (Wei et al. 2019). Briefly, the 15–16 days embryos were removed at and subsequently minced the meninges and vessels under a microscope before separating and shredding the cortex from the cerebrum. The cortex then was digested in pancreatic enzymes for 20 min at 37 °C with gentle shaking every 5 min. The digested neurons were resuspended in NM medium composed of neurobasal medium, 0.5 mM L-glutamine and 2% B27 before being plated onto the Poly-L-Lysine (PLL) pretreated dishes with a density of 1.5×10^6 cells/cm^2. The neurons were cultured in a 5% CO2 incubator at 37 °C, and the culture medium was renewed every 3 days. Microglial BV2 cells and primary cultured neurons were co-cultured using the Transwell (Merck, Darmstadt, Germany) embedded cell co-culture method with the density of 1.5×10^6 cells/cm^2, where primary cultured neurons were planted in the upper chamber and BV2 microglia were planted in the lower layer. NM culture medium was added, and 20μL mouse whole blood was added for 24 h for further experiments. The culture medium was replaced every 3 days.

Lentivirus Construction and Transfection

The LCN2 overexpression and shRNA lentiviruses for overexpression (OE) and interference (IntF) were purchased from HanBio (Shanghai, China). The lentiviruses were preparation as previously described (Fei et al. 2024), and the multiplicity of infections (MOI) is subject to change (Supplemental data).

In Vitro Blood Injury Model

The whole blood of C57BL/6 mice was obtained and added to the cultured cells for certein durations before performing observational tests (including molecular biology tests and morphological experiments), and all cell lines were cultured at 37 °C in a 5% CO_2 incubator while undergoing blood-induced injury.

Mouse Genotype Verification

Mouse tail was digested with proteinase K at 55 °C for 20 min and was further inactivated with proteinase K at 100 °C for 5 min. PCR was performed using the One-Step Mouse Genotyping Kit (Vazyme, Nanjing, China) according to the manufacturer's instructions. Lcn2 primers: F: 5′-TGA TCA TTC TGT GTC CTA GGG GAT G-3′, R: 5′-TTA GCC TCT TCC AAG GCT AGA CAA-3′ (Homozygotes: one band at 203 bp, Heterozygotes: two bands at 203 bp and 144 bp, Wildtype allele: one band at 144 bp). Cx3cr1-Cre primers: F1: 5′-GAC ATT TGC CTT GCT GGA C-3′, R: 5′-GCA GGG AAA TCT GAT GCA AG-3′ (Wildtype: N.A. Targeted: 380 bp).

Antibodies and Drugs

The primary antibodies used in this study included polyclonal goat anti-Iba1 (Abcam, #ab5076, RRID: AB_2224402, 1:400), polyclonal rabbit anti-Iba1 (Abcam, #ab153696, RRID: AB_2889406,1:400), polyclonal rabbit anti-heme oxygenase-1 (Enzo, #SPA-895, RRID: AB_2314637, 1:500), monoclonal rabbit anti-Darpp-32 (Cell Signaling, #2302, RRID: AB_2169007, 1:100), monoclonal mouse anti-NeuN (MERCK, #MAB377, RRID: AB_2298772, 1:400), polyclonal rabbit anti-CD16 (Abcam, #ab87099, RRID: AB_87099, 1:200), monoclonal rabbit anti-iNOS (Abcam, #ab178945, RRID: AB_11042526, 1:200) and polyclonal goat anti-LCN2 (R&D, #AF1857, RRID: AB_355022, 1:200).

The secondary antibodies used for immunofluorescent staining were donkey anti-rabbit IgG (H + L) Alexa Fluor 488 (Abcam, # ab150061, RRID:AB_2571722), donkey anti-rabbit IgG (H + L) Alexa Fluor 594 (Abcam, # ab150076, RRID:AB_2782993), donkey anti-mouse IgG (H + L) Alexa Fluor 488 (Abcam, # ab150105, RRID:AB_2732856), donkey anti-mouse IgG (H + L) Alexa Fluor 594 (Abcam, # ab150108, RRID:AB_2732073), donkey anti-goat IgG (H + L) Alexa Fluor 488(Abcam, # ab150137, RRID:AB_2892985), and donkey anti-goat IgG (H + L) Alexa Fluor 594(Abcam, # ab150136, RRID:AB_2782994), all obtained from Abcam.

In this study, atorvastatin was purchased from Pfizer (New York, NY, USA), and recombinant mouse LCN2 protein was obtained from R&D Systems (Minneapolis, MN, USA, #1857-LC). The dosages of atorvastatin were set as follows: in the in vivo experiment, mice were administered 20 mg/kg/day of atorvastatin daily until the day of euthanasia; in the in vitro experiment, the final concentrations of atorvastatin in the cell culture medium were 2.5 μM, 5 μM, and 10 μM. The dosage of LCN2 protein was 1 μg in the co-injection mouse model.

Flow Cytometry

Fluorescence-activated cell sorter technology was used in this study and the microglia was sorted following the protocol described previously (Fei et al. 2024). Briefly, microglia isolation was conducted following the manufacturer instruction of Adult Brain Dissociation Kit (Miltenyi Biotec, Germany), and the ipsilateral brains were enzymaticly dissociated using MACS Octo Dissociator with Heaters (Miltenyi Biotec) with program 37 °C -ABDK-01. The extracted homogenate was resuspended and centrifuged at 4 °C with 300 g for 10 min. The red blood cells (RBCs) and debris were removed using RBC Removal Solution. The remaining suspension was incubated with FcR Blocking Reagent and then labelled with CD11b-APC antibody at 4 °C in the dark for 15 min before being detected and harvested for the subsequent investigations.

Quantitative Real-Time Polymerase Chain Reaction (qPCR)

qPCR was conducted as previously described (Fei et al. 2022) and the RNA expression level was calculated using GAPDH for internal control. The primer sequences used in this study are: Lcn2-F: GCAGGTGGTACGTTGTGG, Lcn2-R: GTTGTAGTCCGTGGTGGC and GAPDH-F: TTCCTA CCCCCA ATGTGTCC, GAPDH-R: GGTCCTCAGTGT AGCCCAAG.

Immunofluorescence (IF), Immunohistochemistry (IHC) Staining, TUNEL Staining, Protein Extraction, Western Blot (WB) Analysis, HE Staining, Hematoma Size Measurement and Behavioral Tests

The IF, IHC, TUNEL staining, protein extraction, WB, HE staining, hematoma size measurement and behavioral tests were performed as previously described (Wei et al. 2022b). The quantification of the microscopic images used in the current study followed the protocols described previously (Wei et al. 2020). Briefly, the cell counting was performed in a blinded manner: Three images at different areas either in the hematoma or peri-hematoma were obtained at 40 × magnification in each brain section using fluorescence microscope (OLYMPUS,BX63,JAPAN). All the counting was repeated three times and the mean values calculated.

Statistical Analysis

All observations, collections and measurements were performed in a blinded manner and were repeated at least three times. Shapiro–Wilk or Kolmogorov–Smirnov tests were used for normality tests, F test (for Student's t-test) or Brown-Forsythe test and bartlett's test (for one-way

ANOVA) were used for variance homogeneity assessment (Supplemental data), and statistical differences were analyzed using the Student's t-test, one-way analysis of variance (ANOVA), two-way ANOVA, Mann–Whitney test, mixed-effects analysis and non-parametric test. All results are presented as mean ± standard deviation (SD), and nonparametric data are displayed as median ± interquartile range. P value < 0.05 was considered statistically significant.

Results

Atorvastatin Alleviates Neural Damage and Promote Neurological Outcome After Intracerebral Hemorrhage

To investigate the effects of atorvastatin on intracerebral hemorrhage (ICH)-induced neural damage in mice, an ICH model was established. Hematoxylin and eosin (HE) staining of mouse brain tissue was performed, and hematoma volume was measured at days 1 and 7 post-ICH. Results showed that mice in the atorvastatin (Ato) group exhibited significantly smaller hematoma volumes on day 7, but not on day 1, compared to the vehicle (Veh) group (Fig. 1A, B). Terminal deoxynucleotidyl transferase dUTP nick end labeling (TUNEL) staining revealed fewer TUNEL(+) cells in the atorvastatin group than in the vehicle group at day 7 post-ICH (Fig. 1C, D). Forelimb use asymmetry and corner turn tests were conducted before ICH (baseline) and at days 1, 3, and 7 post-ICH. Behavioral deficits were attenuated in the atorvastatin group compared to the vehicle group at day 7, but not at days 1 or 3 (Fig. 1E, F).

Atorvastatin Attenuates Macrophage/Microglia-Related Neuroinflammation

To better understand the role of atorvastatin in microglia/macrophage (M/M)-induced neuroinflammation, we investigated the effects of atorvastatin on M/Ms after intracerebral hemorrhage (ICH) both in vivo and in vitro. First, a BV2-neuron co-culture model was established, followed by induction of blood infusion (BI) injury. A CCK-8 assay of primary neurons revealed that atorvastatin alleviated neuronal death in a concentration-dependent manner (Fig. 2A). Based on cell viability results, an atorvastatin concentration of 5 μM was selected for subsequent in vitro experiments. Immunofluorescence (IF) staining using Iba-1 and CD16, a marker of M1 pro-inflammatory phenotype, demonstrated significantly lower relative CD16 expression in the atorvastatin-treated group compared to the vehicle group after BI injury (Fig. 2B, C). IF staining was also performed to assess morphological changes in primary neurons (Fig. 2D). NeuN(+) cell loss was significantly attenuated, and relative axon length was significantly increased in the atorvastatin group compared to the vehicle group after BI injury (Fig. 2E, F).

To further investigate the role of atorvastatin in microglia/macrophage (M/M)-related neuroinflammation, a mouse intracerebral hemorrhage (ICH) model was established. Immunohistochemical (IHC) staining using M/M activation markers Iba-1 and heme oxygenase-1 (HO-1) revealed that both the number of Iba-1(+) cells and HO-1(+) cell counts were significantly lower in the atorvastatin-treated group compared to the vehicle group at days 3 and 7 post-ICH, but not at day 1 (Fig. 3A–C). Immunofluorescence (IF) staining for Iba-1 and CD16 showed that the count of CD16(+)Iba-1(+) cells was significantly reduced in the atorvastatin group compared to the vehicle group at day 7 post-ICH (Fig. 3D, E). Additionally, peri-hematomal brain tissues were collected for TNF enzyme-linked immunosorbent assay (ELISA), which demonstrated significantly lower TNF secretion in the atorvastatin group compared to the vehicle group (Fig. 3F).

Atorvastatin Inhibits LCN2 Expression After Intracerebral Hemorrhage

The mouse ICH model was established with or without concomitant atorvastatin treatment, and microglia/macrophages (M/Ms) in peri-hematomal brain tissue were sorted via flow cytometry. Western blot (WB) analysis revealed that ICH-induced upregulation of LCN2 expression in M/Ms was significantly attenuated by atorvastatin treatment (Fig. 4A, B). Immunofluorescence (IF) staining using Iba-1 and LCN2 was performed to assess the spatial distribution of LCN2 post-ICH. Results showed that atorvastatin significantly reduced the abundance of LCN2(+)Iba-1(+) cells at day 7 post-ICH (Fig. 4C, D). In vitro, BV2 microglial cells were cultured with varying concentrations of atorvastatin. IF staining for LCN2 and Iba-1 demonstrated that BI injury elevated LCN2 expression in BV2 cells, which was attenuated by atorvastatin in a concentration-dependent manner (Fig. 4E, F). ELISA of cell culture supernatants showed that BI injury-induced LCN2 secretion was similarly reduced by atorvastatin treatment (Fig. 4G). qPCR analysis revealed that Lcn2 mRNA upregulation following BI injury was reversed by atorvastatin in a dose-dependent fashion (Fig. 4H).

Atorvastatin Exerts Anti-neuroinflammation and Neural Protection Effects via Macrophage/Microglia LCN2 Suppression

To further investigate the potential connections between M/Ms LCN2 inhibition and the anti-neuroinflammation effect of atorvastatin after intracerebral hemorrhage (ICH), the M/Ms LCN2 conditional knockout (cKO) mouse model [LCN2fl/fl,cx3cr1-cre] was established and verified. The

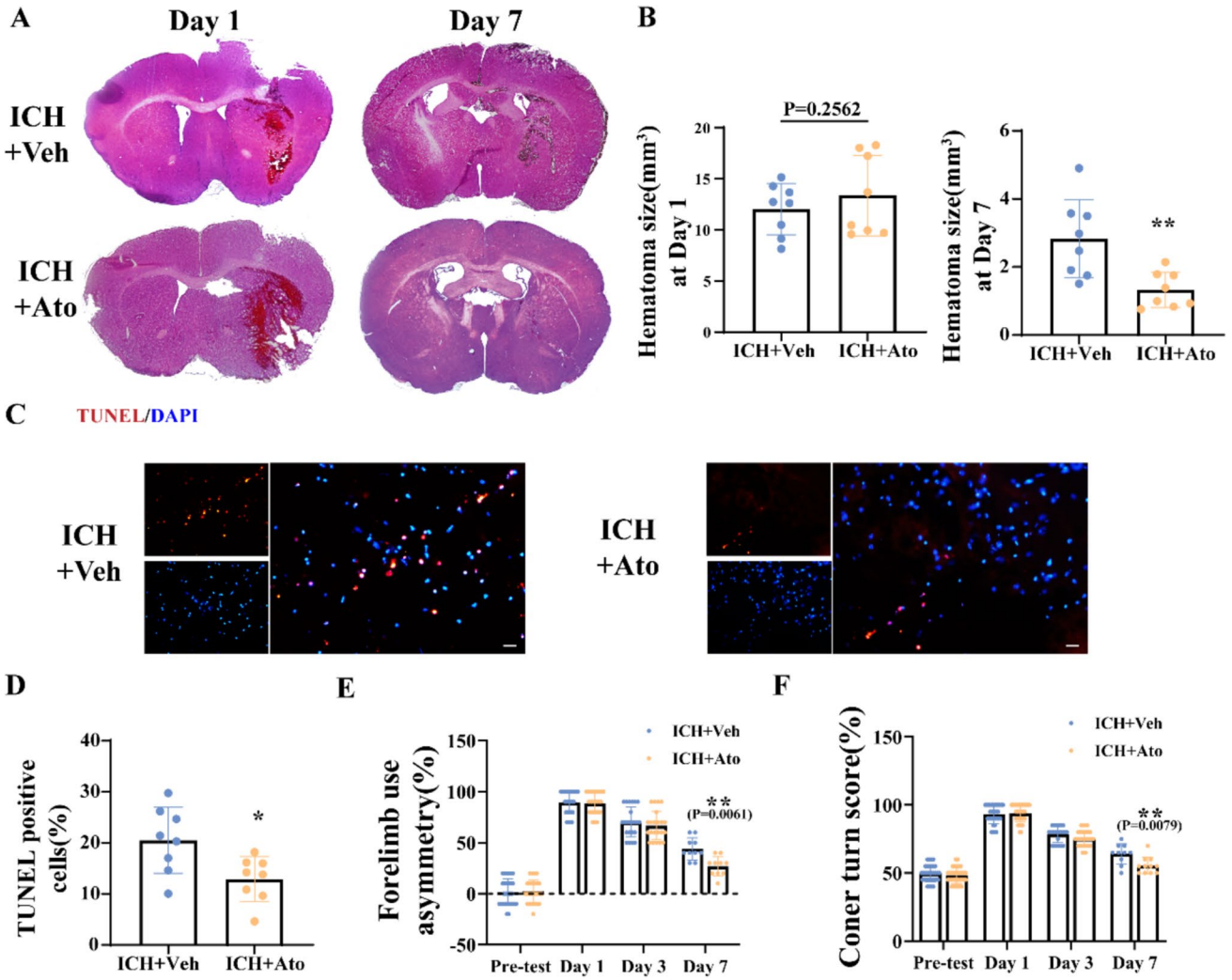

Fig. 1 Atorvastatin alleviates neural damage and promote neurological outcome after intracerebral hemorrhage. **A** HE staining of male mice brains after ICH at days 1 and 7. **B** The size of the hematoma in each group was calculated. For each group, n = 8. Scale bar = 500 μm. t = 0.8096, df = 14, ^{NS}p = 0.2562 for Day 1 and t = 3.370, df = 14, **p = 0.0046 for Day 7. **C** TUNEL images and **D** quantification of the peri-hematomal area in ICH + Veh mice and ICH + Ato mice brains at day 7 after ICH. For each group, n = 8. Scale bar = 20 μm. t = 2.741, df = 14, **p = 0.0159. **E** Forelimb uses asymmetry and **F** corner turn scores before and after ICH in ICH + Veh mice and ICH + Ato mice. n = 24 for each group at pre-ICH and day 1 after ICH, n = 16 at day 3 after ICH and n = 8 for each group at day 7 after ICH. Values are mean ± SD. **p < 0.01 vs. ICH + Veh group by mixed-effects analysis. [$F_{time \times drug}(3, 125) = 3.111$, P = 0.0288 for Forelimb uses asymmetry] [$F_{time \times drug}(3, 189) = 3.109$, P = 0.0276 for corner turn]

immunofluorescence (IF) staining using CD16 and Iba-1 showed that the attenuation effects of atorvastatin on Iba-1(+) M/M activation, the relative expression level of CD16, and the polarization of CD16(+)Iba-1(+) M/Ms were largely abolished by the co-injection of LCN2 protein at day 3 after ICH (Fig. 5A–D). Meanwhile, LCN2 conditional knockout reduced Iba-1(+) M/M activation, lowered the relative expression level of CD16, and inhibited the polarization of CD16(+)Iba-1(+) M/Ms. However, no significant difference was observed between the LCN2 cKO + Vehicle (Veh) mouse and the LCN2 cKO + atorvastatin treatment mouse at day 3 after ICH (Fig. 5A–D).

The LCN2-overexpressing (LCN2-OE) BV2 cell lines, which were infected with lentiviruses at a multiplicity of infection (MOI) of 100, and the LCN2-interfered (LCN2-IntF) BV2 cell lines, which were infected with lentiviruses at an MOI of 50, were constructed and cultured before the establishment of the brain injury (BI) model. The IF staining assay using Iba-1 and inducible nitric oxide synthase (iNOS), another M1 pro-inflammatory phenotype marker, was conducted. The results showed that the addition of LCN2 protein partly reversed the inhibitory effect of atorvastatin on the expression level of iNOS at 24 h after BI injury (Fig. 5E, F). Meanwhile, there was no significant

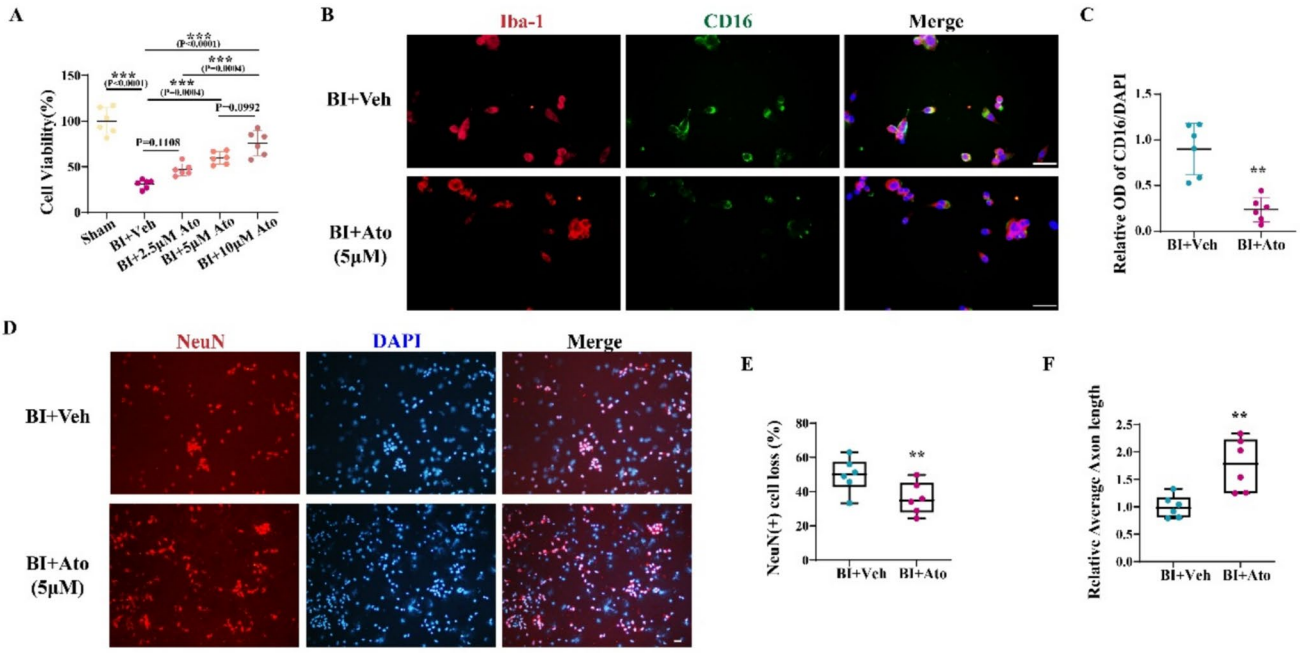

Fig. 2 Atorvastatin inhibits microglia pro-inflammatory polarization and alleviates blood associated primary neuronal damage. **A** CCK-8 assay results of primary neurons collected from BV2-neuron co-culture system with or without different concentrations of atorvastatin treatment 24 h after BI injury. For each group, n = 6. $F(4,25) = 41.79$, ***p < 0.0001 by one-way ANOVA. **B**, **C** Double-immunofluorescence staining of Iba-1 and CD16 in BV2 cell line at 24 h after BI injury. For each group, n = 6. t = 5.196, df = 10, ***p = 0.0004. **D** Immunofluorescence staining of NeuN in primary cultured neurons from BV2-neuron co-culture system at 24 h after BI injury, and the **E** NeuN(+) cell loss and **F** relative axonal length were calculated. For each group, n = 6. t = 2.419, df = 10, *p = 0.0361 for NeuN(+) cell loss and t = 3.590, df = 10, **p = 0.0049 for relative axonal length

difference in the iNOS expression levels between the LCN2 OE group and the LCN2 OE + atorvastatin group (Fig. 5E, G). Also, the iNOS expression level was significantly lower in the LCN2 IntF group than that in the LCN2 negative control (NC) group, but no significant difference was found between the LCN2 IntF group and the LCN2 IntF + atorvastatin group (Fig. 5E, H). The supernatant of the cell culture medium was collected for an enzyme-linked immunosorbent assay (ELISA). The results showed that the addition of LCN2 protein counteracted the effect of atorvastatin on the secretion of interleukin-1β (IL-1β) and tumor necrosis factor (TNF). Moreover, atorvastatin had no significant protective effect on the secretion of IL-1β and TNF after LCN2 overexpression, nor did it provide further protection after LCN2 interference at 24 h after BI injury in the BV2 cell line (Fig. 5I, J).

The role of LCN2 in atorvastatin-induced neural protection after intracerebral hemorrhage (ICH) was also investigated in the present study. The results of the TUNEL assay showed that the number of TUNEL(+) cells was lower in LCN2 cKO mice than in LCN2fl/fl mice. However, no significant difference was observed between the LCN2 cKO mice + Vehicle (Veh) group and the LCN2 cKO mice + atorvastatin group at day 7 after ICH (Fig. 6A, B). The IHC staining of neuron remnants using Darpp32 showed that the loss of Darpp32(+) neurons was lower in LCN2 cKO mice than in LCN2fl/fl mice. Yet, no significant difference was observed between the LCN2 cKO mice + Veh group and the LCN2 cKO mice + atorvastatin group at day 28 after ICH (Fig. 6C, D). The forelimb use asymmetry and corner turn test results of each mouse were recorded. The results indicated that the behavioral deficits were more attenuated in LCN2 cKO mice than in LCN2fl/fl mice. Nevertheless, no significant difference was observed between the LCN2 cKO mice + Veh group and the LCN2 cKO mice + atorvastatin group at day 7 after ICH (Fig. 6E, F). The LCN2 overexpression and negative-control BV2 cell lines were constructed and cultured. The results of the NeuN staining assay showed that the loss of NeuN(+) cells and the relative axonal shrinkage were significantly more attenuated in the LCN2 NC + atorvastatin group than in the LCN2 NC group after brain injury (BI). This effect was significantly reversed by LCN2 overexpression (Fig. 6G–I).

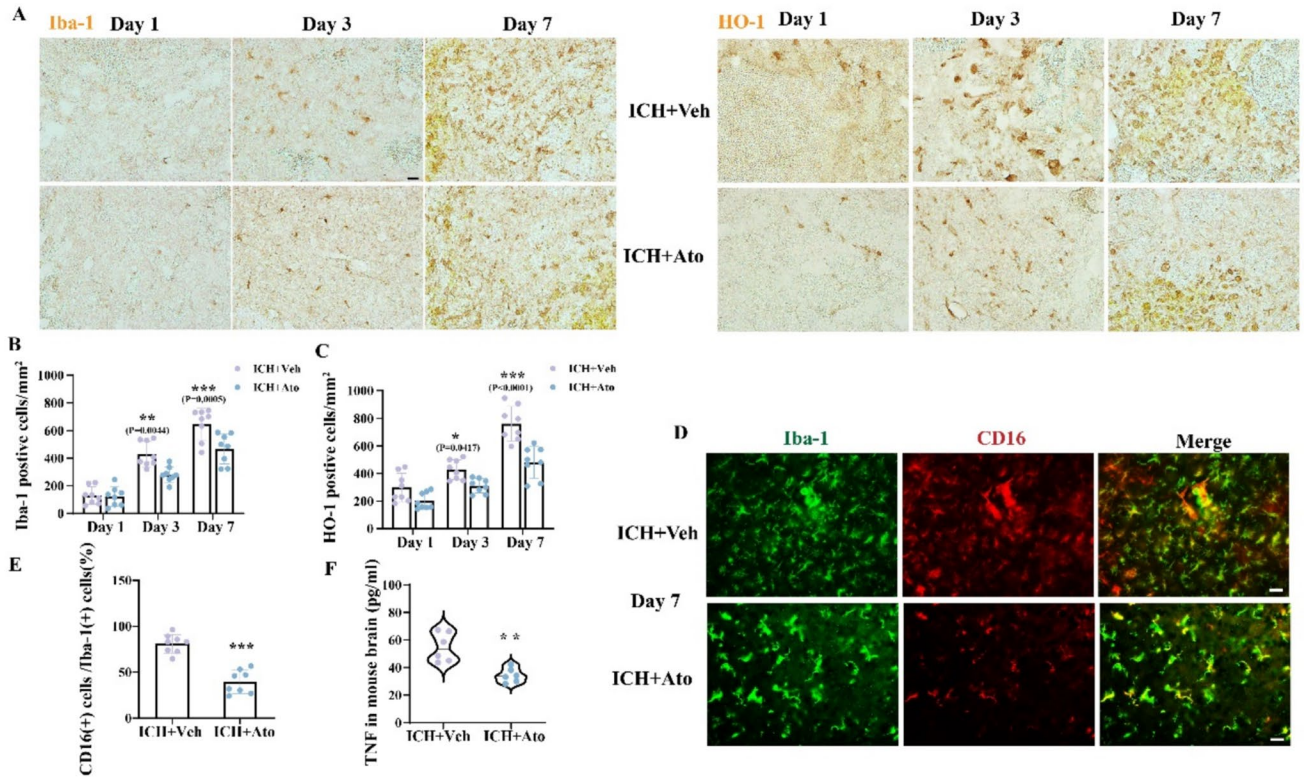

Fig. 3 Atorvastatin inhibits macrophage/microglia activation, M1 polarization and pro-inflammatory cytokine release. **A** Immunohistochemistry staining of Iba-1 and HO-1 at different time points after ICH in ICH + Veh mice and ICH + Ato mice, and the quantifications were presented in **B** and **C** respectively. For each group, n = 8. Scale bar = 20 μm. [$F_{time \times drug}(2, 42) = 4.479$, $P = 0.0173$ for Iba-1] [$F_{time \times drug}(2, 42) = 4.790$, $P = 0.0134$ for HO-1] by two-way ANOVA. **D** Double-immunofluorescence staining of Iba-1 and CD16 in peri-hematomal area of mice brain at day 7 after ICH and the quantifications were presented in **E**. For each group, n = 8. t = 7.246, df = 14, ****p < 0.0001. **F** TNF ELISA assay of brain tissues collected from peri-hematoma area in mice. n = 6. t = 4.271, df = 10, *p = 0.0016

Discussion

The present study investigates the role of M/Ms LCN2 in the anti-inflammatory and neural protective effects of atorvastatin treatment after ICH. Our results demonstrate that the atorvastatin treatment suppresses M/Ms activation, inhibits inflammatory cytokines release, alleviates neural death, facilitates hematoma clearance and improves neurological recovery. Furthermore, our results using transgenic mice unveiled a potential mechanism whereby the protective effects of atorvastatin treatment after ICH are partially attributed to LCN2 signaling inhibition.

Previous studies found that atorvastatin reduced microglia activation and prevented neuronal loss in a collagenase model (Chen et al. 2022). Low dose (2 mg/kg) atorvastatin facilitated vascular recovery and improved the neurological outcome after ICH, but no significant acute-phase hematoma volume change was observed, nor was the detailed mechanism investigated (Yang et al. 2011; Karki et al. 2009). Recent studies have shown that high dose (20 mg/kg) atorvastatin exhibits prominent anti-cardiotoxicity effect, indicating promising potential for high-dose intervention (Efentakis et al. 2024). In the current study, 20 mg/kg/d atorvastatin treatment significantly reduced hematoma size, alleviated neural death and preserved neurologic function in hemorrhagic mice, suggesting a neuroprotective role of atorvastatin in ICH. Neuroinflammation activation is a key mechanism of secondary brain injury after ICH, in which the activation of in-situ microglia and peripheral macrophages plays pivotal roles (Wei et al. 2022b). The M/Ms exhibit pro-inflammatory phenotype marked by CD16 and iNOS, secreting pro-inflammatory injury factors such as IL-1, IL-6 and TNF, which are important mechanisms of brain injury after ICH (Lan et al. 2017). Our current study shows that high-dose atorvastatin effectively alleviates the expression level of the M1 polarization marker CD16 in BV2 microglia after blood infusion and down-regulates the secretion level of pro-inflammatory cytokines into the culture supernatant. In addition, results from a microglia-neuron co-culture experiment suggest that atorvastatin inhibits neuronal cell death and preserves axonal morphology after blood infusion. Furthermore, our in vivo results show that atorvastatin intervention significantly reduces Iba-1(+) and HO-1(+)

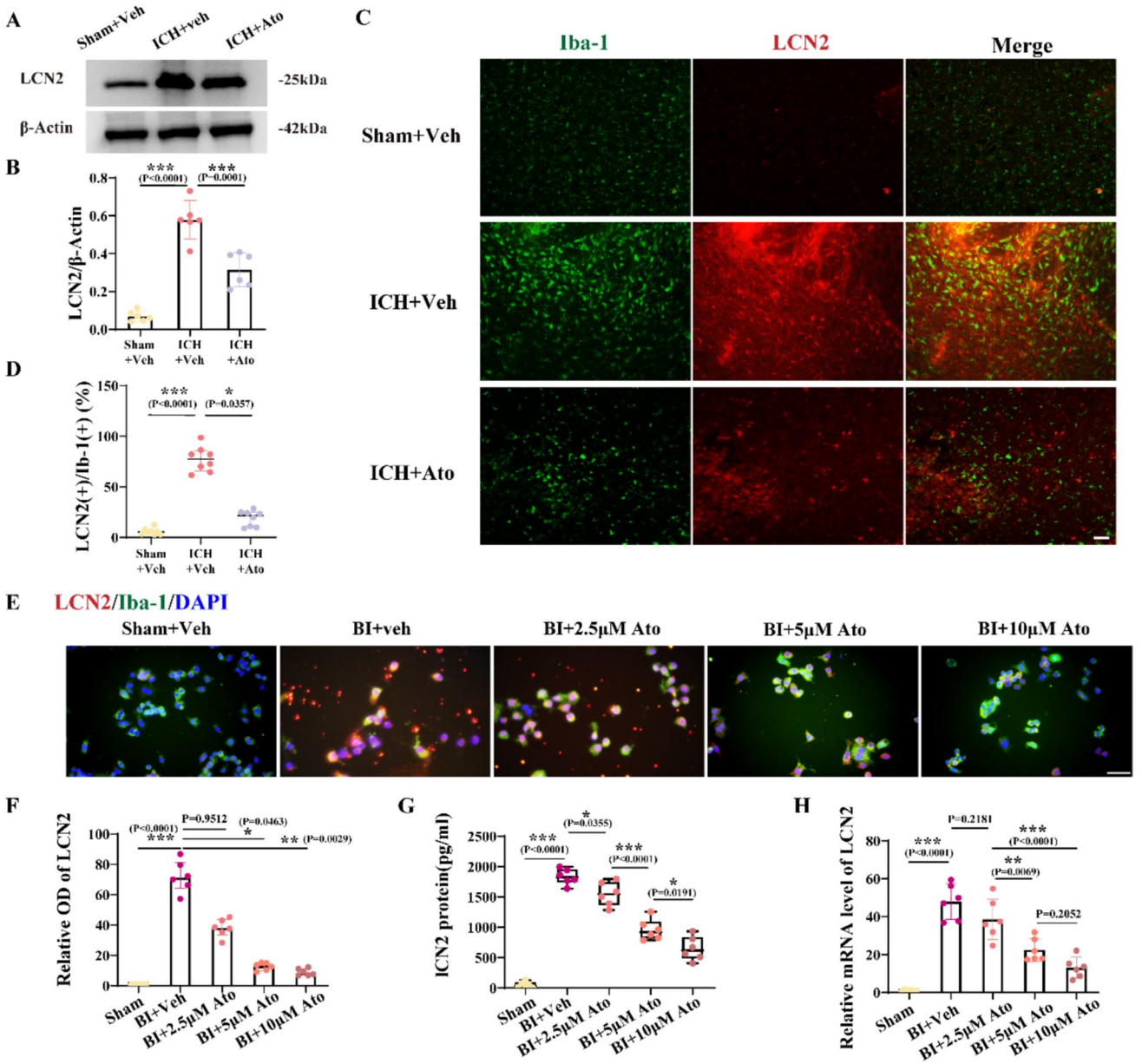

Fig. 4 Atorvastatin inhibits macrophage/microglia LCN2 expression after ICH and microglia LCN2 expression after BI injury. **A** The macrophage/microglia were sorted from mice hemorrhagic brain via flow cytometry, from which the protein was extracted before conducting western blot assay. **B** The quantification of each blot was calculated. For each group, n = 6. F(2,15) = 61.19, ***p < 0.0001 by one-way ANOVA. **C** Double-immunofluorescence staining of Iba-1 and LCN2 in peri-hematomal area of mice brain at day 3 after ICH and the quantifications were presented in **D**. For each group, n = 8. Data are displayed as median ± interquartile range. Z = 4.419, ***p < 0.0001 for Sham + Veh vs ICH + Veh and Z = 2.369, *p < 0.0357 for ICH + Veh vs ICH + ATo by non-parametric test(Kruskal–Wallis). **E** Double-immunofluorescence staining of Iba-1 and LCN2 in BV cell line at 24 h after BI injury and the quantifications were presented in **F**. For each group, n = 6. Data are displayed as median ± interquartile range. Z = 4.722, ***p < 0.0001 for Sham + Veh vs BI + Veh, Z = 1.180, p = 0.9512 for BI + Veh vs BI + 2.5 μM Ato, Z = 2.525, *p = 0.0463 for BI + Veh vs BI + 5 μM Ato and Z = 3.378, **p = 0.0029 for BI + Veh vs BI + 10 μM Ato by non-parametric test(Kruskal–Wallis). **G** ELISA assay results of LCN2 from supernatant of BV2 culture medium. n = 6. F(4,25) = 120.8, ***p < 0.0001 by one-way ANOVA. **H** qPCR analysis of relative mRNA levels of *Lcn2* in BV2 cell lines. For each group, n = 6. F(4,25) = 39.68, ***p < 0.0001 by one-way ANOVA

M/Ms activation, lowers M1 marker CD16 expression, and down-regulates TNF levels in the hemorrhagic brain. These results suggest that atorvastatin treatment attenuates M/Ms-related neuroinflammation after ICH.

Atorvastatin has been found to effectively alleviate the expression of the inflammatory protein LCN2 and improve disease prognosis in other diseases (Kang et al. 2020; Park et al. 2016; Torrens et al. 2009). Our previous

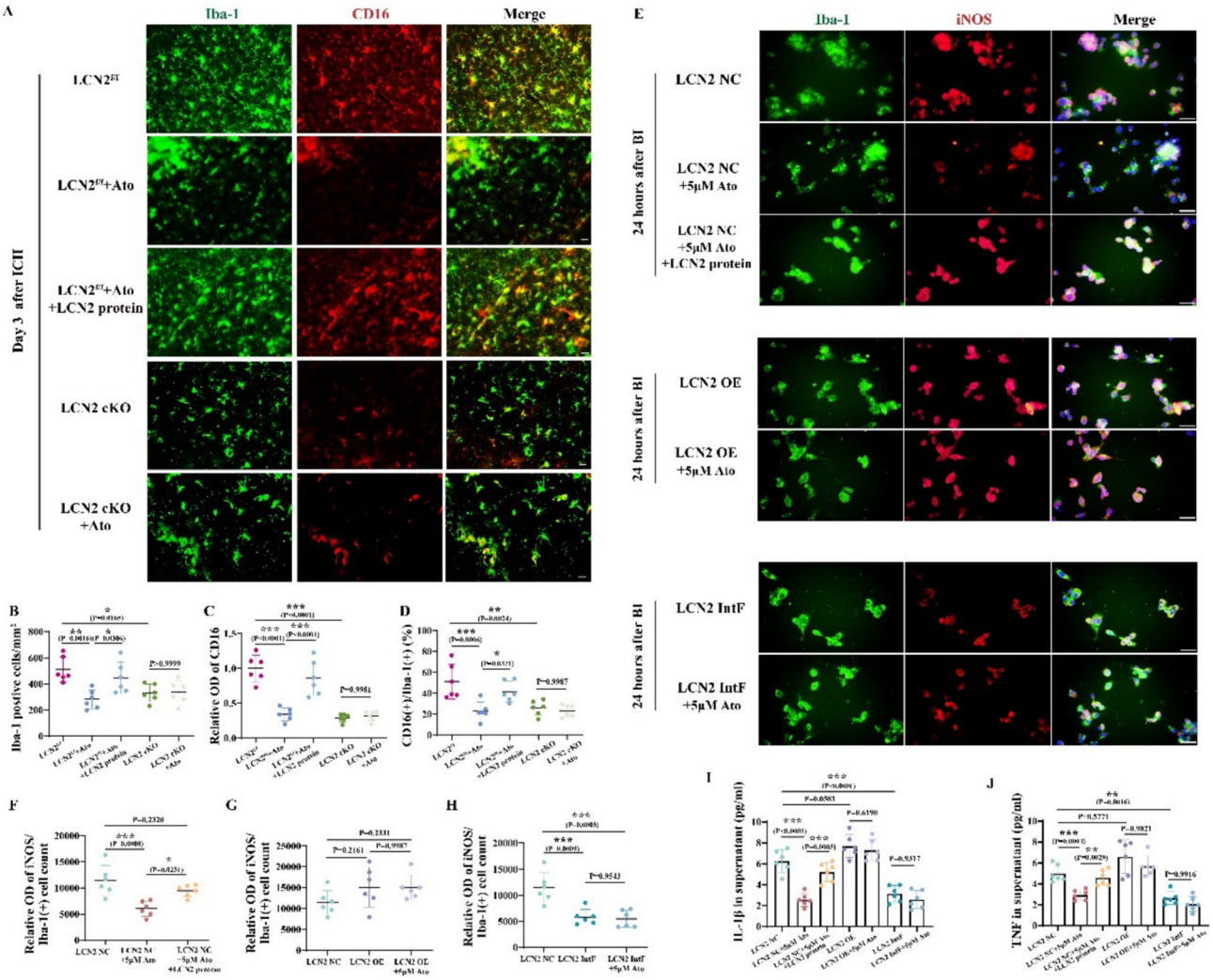

Fig. 5 Atorvastatin exerts anti-neuroinflammation via macrophage/microglia LCN2 suppression. **A** Double-immunofluorescence staining of Iba-1 and CD16 in peri-hematoma area of mice brain at day 3 after ICH and the quantifications for Iba-1(+) cell count (**B**), relative OD of CD16 (**C**) and CD16(+)Iba-1(+) cell percentage **D** were presented. For each group, n = 6. $F(4,25) = 6.471$, $^{**}p = 0.0010$ for Iba-1(+) cell count, $F(4,25) = 30.07$, $^{***}p < 0.0001$ for relative OD of CD16 and $F(4,25) = 9.163$, $^{***}p = 0.0001$ for CD16(+)Iba-1(+) cell percentage by one-way ANOVA. **E** Double-immunofluorescence staining of Iba-1 and iNOS in BV cell line at 24 h after BI injury and the quantifications of iNOS OD values in different comparisons were presented in **F**–**H**. $F(2,15) = 11.39$, $^{**}p = 0.0010$ for **F**, $F(2,15) = 2.012$, $p = 0.1683$ for **G** and $F(2,15) = 15.153$, $^{***}p = 0.0003$ for **H** by one-way ANOVA. IL-1β (**I**) and TNF (**J**) ELISA assays for supernatant from cell culture medium were conducted. n = 6. $F(6,35) = 34.14$, $^{***}p < 0.0001$ for IL-1β and $F(6,35) = 20.35$, $^{***}p < 0.0001$ for TNF by one-way ANOVA

studies have shown that LCN2 is highly expressed in peri-hematomal M/Ms, and inhibition of LCN2 expression alleviates neural damage caused by M/Ms-mediated neuroinflammation and promotes neural recovery after ICH (Fei et al. 2024). To further explore whether LCN2 is involved in the anti-inflammatory effect of atorvastatin after ICH, we measured the expression level of LCN2 with or without atorvastatin treatment. Western blot results showed that the expression level of LCN2 protein in the peri-hematoma region of the mouse brain was significantly down-regulated after atorvastatin treatment, and immunofluorescence staining results indicated that the expression level of LCN2 in M/Ms was significantly lower in the atorvastatin-treated group than in the vehicle group. In addition, our in vitro results showed that the down-regulation effect of atorvastatin on LCN2 expression exhibits a dose-dependent manner, as demonstrated by immunocytochemistry, PCR, and ELISA results. Collectively, these results suggest that atorvastatin treatment counteracts the upregulation of LCN2 expression after ICH.

To further explore whether LCN2 inhibition is the key mechanism by which atorvastatin alleviates neuroinflammation after ICH, we established the LCN2 protein co-injection

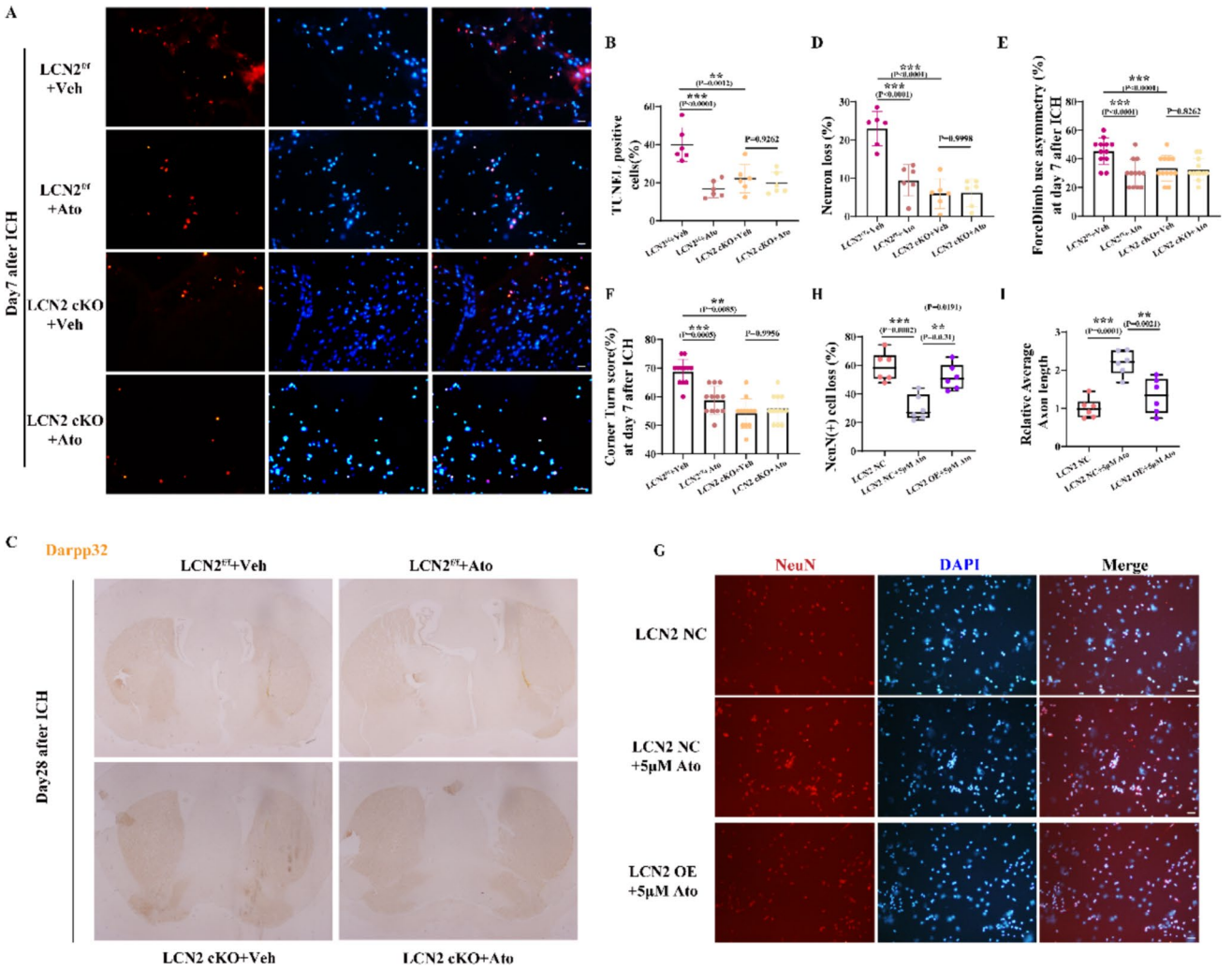

Fig. 6 Atorvastatin alleviates neural damage and neurological deficit via macrophage/microglia LCN2 downregulation. **A** TUNEL images and **B** quantification of the peri-hematomal area in mice from different groups at day 7 after ICH. For each group, n = 6. Scale bar = 20 μm. $F(3,20) = 13.90$, ***$p < 0.0001$ by one-way ANOVA. **C** Immunohistochemistry staining of Darpp32 in mouse brain from different groups at day 28 after ICH, and the neuronal loss(%) was calculated and presented **D** by equation: neuron loss = Area(ipsilateral)/Area(contralateral)*100(%). For each group, n = 6. $F(3,20) = 24.06$, ***$p < 0.0001$ by one-way ANOVA. **E** Forelimb uses asymmetry and **F** corner turn scores in mice from different groups at day 7 after ICH. n = 12. Values are mean ± SD. $F(3,44) = 7.327$, ***$p = 0.0004$ for forelimb use asymmetry and $F(3,44) = 22.61$, ***$p < 0.0001$ for corner turn scores by one-way ANOVA. **G** Immunofluorescence staining of NeuN in primary cultured neurons from BV2-neuron co-culture system at 24 h after BI injury in LCN2 NC group, LCN2 NC + Ato group and LCN2 OE + Ato group, and the **H** NeuN(+) cell loss and **I** relative axonal length were calculated. For each group, n = 6. $F(2,15) = 15.41$, ***$p = 0.0002$ for NeuN(+) cell loss and $F(2,15) = 17.75$, ***$p = 0.0001$ for relative axonal length by one-way ANOVA

ICH model described previously (Fei et al. 2024). Results suggested that LCN2 recombinant protein injection reversed the inhibitory effect of atorvastatin on M1 polarization. To further investigate the role of M/Ms-specific LCN2 in atorvastatin's anti-inflammation, LCN2f/f, CX3CR1-Cre mice were used in the current study. Results indicated that atorvastatin treatment had no anti-M1 polarization effects in LCN2-specific knockout mice. Similarly, our in vitro model showed that LCN2 recombinant protein or LCN2 overexpression reversed the inhibitory effect of atorvastatin on microglial M1 polarization and the secretion of inflammatory factors IL-1β and TNF, while LCN2 interference largely abolished the anti-M1 polarization effect of atorvastatin. These results suggest that atorvastatin can relieve M/Ms-induced neuroinflammation after intracerebral hemorrhage by down-regulating LCN2 expression. Furthermore, we investigated the role of LCN2 in atorvastatin-induced neuroprotection after ICH. TUNEL results suggested that atorvastatin significantly alleviates neural death in LCN2f/f mouse brains. Darpp32 staining results showed that atorvastatin

effectively preserves neuron survival levels in the ipsilateral basal ganglia of LCN2f/f mouse brains 4 weeks after ICH, and functional test results showed better neurological outcomes in the atorvastatin treatment group, suggesting significant neuroprotective effects of atorvastatin after ICH in LCN2f/f mice. However, such protective effects of atorvastatin were not observed in M/M LCN2-specific knockout mice, indicating that LCN2 inhibition is the key mechanism of atorvastatin-induced neuroprotection after ICH. This conclusion is also supported by in vitro experiments, where the neuron survival and morphological preservation effects of atorvastatin were abolished by LCN2 overexpression.

However, our experimental results showed no significant change between $LCN2^{f/f}$ + Ato group and the LCN2 cKO + Ato group (Supplemental Figure S1), indicating that the pro-hematoma-clearance effect of Atorvastatin may not be attributed to the LCN2 inhibition. Further studies are needed to investigate the mechanism underlying Ato-induced hematoma clearance. Additionally, since atorvastatin is a major cholesterol-lowering agent, further studies are needed to explore the potential relationship between ICH and cholesterol biosynthesis.

In conclusion, our results demonstrate that atorvastatin treatment attenuates macrophage/microglia-related neuroinflammation and protects neural recovery after ICH. This study identifies a potential novel target for ICH treatment.

There are several limitations to the current study: 1. Only young male mice were used, and further studies focusing on female and old mice are needed. 2. No a priori sample size calculation was performed in the current study. 3. High dose of atorvastatin was tested in the present study, and further studies are needed to investigate the potential side effects of atorvastatin use for ICH and to determine the optimized dose for clinical translation. 4. The specificity of the antibodies used in the current study was not determined.

Supplementary Information The online version contains supplementary material available at https://doi.org/10.1007/s10571-025-01566-w.

Author Contributions GMW and HKH performed animal experiment and drafted the manuscript. JBL performed the in vitro experiment. XWF and YND collected and analyzed the data. LY and LW participated in animal behavioral tests. YY and GHH participated in the data analysis. DFZ revised the manuscript. LJ and JLW conceived the study idea and supervised the study.

Funding This study was supported by National Natural Science Foundation of China (No. 82101374, No. 82401720).

Data Availability No datasets were generated or analysed during the current study.

Declarations

Conflict of interest All authors declare that they have no conflict of interest.

Ethical Approval All institutional and national guidelines for the care and use of laboratory animals were followed.

References

Castellano JM, Pocock SJ, Bhatt DL, Quesada AJ, Owen R, Fernandez-Ortiz A, Sanchez PL, Marin Ortuno F, Vazquez Rodriguez JM, Domingo-Fernandez A et al (2022) Polypill strategy in secondary cardiovascular prevention. N Engl J Med 387:967–977

Chen J, Zhang C, Yan T, Yang L, Wang Y, Shi Z, Li M, Chen Q (2021) Atorvastatin ameliorates early brain injury after subarachnoid hemorrhage via inhibition of pyroptosis and neuroinflammation. J Cell Physiol 236:6920–6931

Chen D, Sui L, Chen C, Liu S, Sun X, Guan J (2022) Atorvastatin suppresses NLRP3 inflammasome activation in intracerebral hemorrhage via TLR4- and MyD88-dependent pathways. Aging (Albany NY) 14:462–476

Dekens DW, Eisel ULM, Gouweleeuw L, Schoemaker RG, De Deyn PP, Naude PJW (2021) Lipocalin 2 as a link between ageing, risk factor conditions and age-related brain diseases. Ageing Res Rev 70:101414

Efentakis P, Choustoulaki A, Kwiatkowski G, Varela A, Kostopoulos IV, Tsekenis G, Ntanasis-Stathopoulos I, Georgoulis A, Vorgias CE, Gakiopoulou H et al (2024) Early microvascular coronary endothelial dysfunction precedes pembrolizumab-induced cardiotoxicity. Preventive role of high dose of atorvastatin. Basic Res Cardiol 120:263

Fassett RG, Robertson IK, Ball MJ, Geraghty DP, Cardinal JW, Coombes JS (2012) Effects of atorvastatin on NGAL and cystatin C in chronic kidney disease: a post hoc analysis of the LORD trial. Nephrol Dial Transplant 27:182–189

Fei X, Dou YN, Wang L, Wu X, Huan Y, Wu S, He X, Lv W, Wei J, Fei Z (2022) Homer1 promotes the conversion of A1 astrocytes to A2 astrocytes and improves the recovery of transgenic mice after intracerebral hemorrhage. J Neuroinflammation 19:67

Fei X, Dou Y, Yang Y, Zheng B, Luo P, Dai S, Zhang J, Peng K, Jiang X, Yu Y et al (2024) Lipocalin-2 inhibition alleviates neural injury by microglia ferroptosis suppression after experimental intracerebral hemorrhage in mice via enhancing ferritin light chain expression. Biochim Biophys Acta Mol Basis Dis 1870:167435

Gaist D, Garcia Rodriguez LA, Hallas J, Hald SM, Moller S, Hoyer BB, Selim M, Goldstein LB (2023) Association of statin use with risk of stroke recurrence after intracerebral hemorrhage. Neurology 101:e1793–e1806

Gao Y, Jiang L, Pan Y, Chen W, Jing J, Wang C, Johnston SC, Amarenco P, Bath PM, Yang Y et al (2024) Immediate- or delayed-intensive statin in acute cerebral ischemia: the INSPIRES randomized clinical trial. JAMA Neurol 81:741–751

Goldberg G, Coelho L, Mo G, Adang LA, Patne M, Chen Z, Garcia-Bassets I, Mesci P, Muotri AR (2024) TREX1 is required for microglial cholesterol homeostasis and oligodendrocyte terminal differentiation in human neural assembloids. Mol Psychiatry 29:566–579

Hu S, Zhu Y, Zhao X, Li R, Shao G, Gong D, Hu C, Liu H, Xu K, Liu C et al (2023) Hepatocytic lipocalin-2 controls HDL metabolism and atherosclerosis via Nedd4-1-SR-BI axis in mice. Dev Cell 58(2326–2337):e2325

Iadecola C, Buckwalter MS, Anrather J (2020) Immune responses to stroke: mechanisms, modulation, and therapeutic potential. J Clin Invest 130:2777–2788

Kang J, Sun Y, Deng Y, Liu Q, Li D, Liu Y, Guan X, Tao Z, Wang X (2020) Autophagy-endoplasmic reticulum stress inhibition mechanism of superoxide dismutase in the formation of calcium oxalate kidney stones. Biomed Pharmacother 121:109649

Karki K, Knight RA, Han Y, Yang D, Zhang J, Ledbetter KA, Chopp M, Seyfried DM (2009) Simvastatin and atorvastatin improve neurological outcome after experimental intracerebral hemorrhage. Stroke 40:3384–3389

Lan X, Han X, Li Q, Yang QW, Wang J (2017) Modulators of microglial activation and polarization after intracerebral haemorrhage. Nat Rev Neurol 13:420–433

Li X, Wang X, Guo L, Wu K, Wang L, Rao L, Liu X, Kang C, Jiang B, Li Q et al (2023) Association between lipocalin-2 and mild cognitive impairment or dementia: a systematic review and meta-analysis of population-based evidence. Ageing Res Rev 89:101984

Liu Y, Shao YH, Zhang JM, Wang Y, Zhou M, Li HQ, Zhang CC, Yu PJ, Gao SJ, Wang XR et al (2023) Macrophage CARD9 mediates cardiac injury following myocardial infarction through regulation of lipocalin 2 expression. Signal Transduct Target Ther 8:394

Neilan TG, Quinaglia T, Onoue T, Mahmood SS, Drobni ZD, Gilman HK, Smith A, Heemelaar JC, Brahmbhatt P, Ho JS et al (2023) Atorvastatin for anthracycline-associated cardiac dysfunction: the STOP-CA randomized clinical trial. JAMA 330:528–536

Park JH, Shim JK, Song JW, Soh S, Kwak YL (2016) Effect of atorvastatin on the incidence of acute kidney injury following valvular heart surgery: a randomized, placebo-controlled trial. Intensive Care Med 42:1398–1407

Prowle JR, Calzavacca P, Licari E, Ligabo EV, Echeverri JE, Haase M, Haase-Fielitz A, Bagshaw SM, Devarajan P, Bellomo R (2012) Pilot double-blind, randomized controlled trial of short-term atorvastatin for prevention of acute kidney injury after cardiac surgery. Nephrology (Carlton) 17:215–224

Puy L, Parry-Jones AR, Sandset EC, Dowlatshahi D, Ziai W, Cordonnier C (2023) Intracerebral haemorrhage. Nat Rev Dis Primers 9:14

Saliba W, Rennert HS, Barnett-Griness O, Gronich N, Molad J, Rennert G, Auriel E (2018) Association of statin use with spontaneous intracerebral hemorrhage: a cohort study. Neurology 91:e400–e409

Torrens C, Kelsall CJ, Hopkins LA, Anthony FW, Curzen NP, Hanson MA (2009) Atorvastatin restores endothelial function in offspring of protein-restricted rats in a cholesterol-independent manner. Hypertension 53:661–667

Toyota Y, Wei J, Xi G, Keep RF, Hua Y (2019) White matter T2 hyperintensities and blood-brain barrier disruption in the hyperacute stage of subarachnoid hemorrhage in male mice: the role of lipocalin-2. CNS Neurosci Ther 25:1207–1214

Vizcaychipi MP, Watts HR, O'Dea KP, Lloyd DG, Penn JW, Wan Y, Pac-Soo C, Takata M, Ma D (2014) The therapeutic potential of atorvastatin in a mouse model of postoperative cognitive decline. Ann Surg 259:1235–1244

Wan Y, Holste KG, Hua Y, Keep RF, Xi G (2023) Brain edema formation and therapy after intracerebral hemorrhage. Neurobiol Dis 176:105948

Wang M, Xia F, Wan S, Hua Y, Keep RF, Xi G (2021) Role of complement component 3 in early erythrolysis in the hematoma after experimental intracerebral hemorrhage. Stroke 52:2649–2660

Wei J, Wu X, Luo P, Yue K, Yu Y, Pu J, Zhang L, Dai S, Han D, Fei Z (2019) Homer1a attenuates endoplasmic reticulum stress-induced mitochondrial stress after ischemic reperfusion injury by inhibiting the PERK pathway. Front Cell Neurosci 13:101

Wei J, Wang M, Jing C, Keep RF, Hua Y, Xi G (2020) Multinucleated giant cells in experimental intracerebral hemorrhage. Transl Stroke Res 11:1095–1102

Wei C, Wang J, Foster LD, Yeatts SD, Claudia Moy J, Mocco MS, Palesch Y, Griffin J, Perlmutter A, Norton C, Dillon C, Thornhill A, Greenberg S, Morgenstern L, Hanley D, Xi G, Bleck TP, Balk R, Palesch Y, Griffin J, Thornhill A, Perlmutter A, Dillon C, Zhao W, Kim J, Kumar S, Norton C, Farinella M, Siwila-Sackman E, Feigert C, Schlaug G, Wang J, Wright C, Janis S, Gilbert P, Kase CS, Carson S, Flaherty M, Kessler CM, McClure LA, Bannon D, Broderick J, Dill A (2022a) Effect of deferoxamine on outcome according to baseline hematoma volume: a post hoc analysis of the i-DEF trial. Stroke 53:1149–1156

Wei J, Dai S, Pu C, Luo P, Yang Y, Jiang X, Li X, Lin W, Fei Z (2022b) Protective role of TLR9-induced macrophage/microglia phagocytosis after experimental intracerebral hemorrhage in mice. CNS Neurosci Ther 28:1800–1813

Yang D, Knight RA, Han Y, Karki K, Zhang J, Ding C, Chopp M, Seyfried DM (2011) Vascular recovery promoted by atorvastatin and simvastatin after experimental intracerebral hemorrhage: magnetic resonance imaging and histological study. J Neurosurg 114:1135–1142

Yang S, Yuan Z, Zhu Y, Liang C, Chen Z, Zhang J, Leng L (2024) Multi-omics analysis reveals GAPDH posttranscriptional regulation of IFN-gamma and PHGDH as a metabolic checkpoint of microglia polarization. Brain Behav Immun 117:155–166

Ye D, Yang K, Zang S, Lin Z, Chau HT, Wang Y, Zhang J, Shi J, Xu A, Lin S et al (2016) Lipocalin-2 mediates non-alcoholic steatohepatitis by promoting neutrophil-macrophage crosstalk via the induction of CXCR2. J Hepatol 65:988–997

Zhang W, Liu Y, Wang Z, He S, Liu W, Wu Y, Yang L, Hu C, Wang Y (2024) Remodeling brain pathological microenvironment to lessen cerebral ischemia injury by multifunctional injectable hydrogels. J Control Release 369:591–603

Zhao H, Garton T, Keep RF, Hua Y, Xi G (2015) Microglia/macrophage polarization after experimental intracerebral hemorrhage. Transl Stroke Res 6:407–409